https://doi.org/10.5194/egusphere-2026-725
Preprint. Discussion started: 16 February 2026

Synoptic drivers of the August 2024 record-breaking rainfall in the Chadian Sahara: Dynamics, thermodynamics, and socio-economic consequences

Claudin Wamba Tchinda[1]· Fréderic Saha[2,3]· Alain T. Tamoffo[4]

[1]Climate Laboratory for Environmental Modeling and Atmospheric Physics (LEMAP), Faculty of Science, University of Yaoundé 1, Yaoundé, Cameroon
[2]Faculty of Arts, Letters and Social Sciences, University of Yaoundé 1, Yaoundé, Cameroon
[3]Community Resilience Association (RESCOM-Tchad), Moundou, Chad
[4]Climate Service Center Germany (GERICS), Helmholtz-Zentrum Hereon, Hamburg, Germany

Corresponding author: Claudin Wamba Tchinda wambatchindaclaudin@yahoo.fr

Claudin Wamba Tchinda's orcid: https://orcid.org/0009-0007-5715-5897
E-mail: wambatchindaclaudin@yahoo.fr

Fréderic Saha's ORCID: 0000-0003-0327-9417
fredericsaha72@gmail.com

Alain T. Tamoffo's ORCID: 0000-0001-8482-8881
alaintamoffotchio@gmail.com

3

Abstract

This study examines the atmospheric mechanisms behind the extreme rainfall event of August 2024 in the northen Chad, and their devastating socio-economic impacts. Analysis of the hydro-climatic regime over the region reveals a major structural transition marked by a statistical tipping point in 2003, shifting from historical aridity to a phase of intensified rainfall that culminated in the record high of August 2024. Our analysis of lower-tropospheric convergence, specific humidity, vertical velocity (ω), and moist static energy (MSE) reveals a major shift from the typical West African monsoon regime. In August 2024, the Intertropical Front (ITF) shifted abnormally northward, reaching 20-22°N, which allows moist moisture air to penetrate deep into the Saharan zone. This shift was driven by strengthened convergence at 850 hPa and a significant increase in low-level humidity. Furthermore, negative ω anomalies throughout the troposphere indicate a northward extension of the monsoon's upward branch. Strong positive MSE anomalies over desert regions further highlight a thermodynamic enrichment of the atmospheric column. Together, these signals point to a highly effective dynamic-thermodynamic coupling that fueled intense convective systems. Ultimately, the synchronization between these atmospheric condition and the synoptic forcing of African easterly waves generated local rainfall anomalies exceeding 100%, redefining the hydrological balance of the Lake Chad basin between aquifer recharge and increased risks of flash flooding. This hydro-climatic shift had immediate and devastating socio-economic impacts: the resulting flooding affected nearly 20,000 people across four desert provinces in Chad. In Tibesti alone, sixty lives were lost due to drowning or building collapses, alongside significant losses of livestock and infrastructure.

Keywords: Chad, extreme rainfall, flooding, intertropical front, west African monsoon, impact

4

https://doi.org/10.5194/egusphere-2026-725
Preprint. Discussion started: 16 February 2026

5

1. Introduction

Extreme precipitation episodes constitute one of the most critical manifestations of contemporary climate variability, posing a growing challenge to the resilience of human societies (Seneviratne et al., 2021). Their impact is particularly devastating in arid and semi-arid regions, where structural water scarcity renders natural and socio-economic systems extremely vulnerable to hydrometeorological anomalies (Saha et al., 2020). Under global warming, the intensification of the hydrological cycle has led to a documented increase in the frequency and magnitude of these events, often exceeding local adaptive capacities (Allan and Soden, 2008; Trenberth et al., 2015; Ehtasham et al., 2024; Adeyeri, 2025). Specifically, surpassing critical warming thresholds could increase intense precipitation in Central Africa by up to 25%, exacerbating flooding risks and population exposure (Zakariahou et al., 2024). This vulnerability is especially concerning for the Lake Chad Basin, where projections indicate a resurgence of rainfall extremes alongside an extension of dry spells (Adeyeri et al., 2019).

The Sahara and its southern margins operate under a climatic regime traditionally governed by tropospheric subsidence and erratic rainfall. In this environment, intense rain events arise from exceptional atmospheric configurations linked to the dynamics of the Saharan Heat Low (SHL) and regional moisture convergence (Selami et al., 2021). This dynamics is part of arainfall recovery observed since the end of the 20th century, driven by oceanic warming and a strengthened monsoon moisture budget (Sindikubwabo et al., 2018; Biasutti, 2019). However, paleoclimatic records serve as a reminder that this system is prone to non-linear and abrupt responses; the history of "Lake Mega-Chad" demonstrates that transitions between aridity and "African Humid Periods" can be sudden (Simon et al., 2015; Pausata et al., 2017; Pausata et al., 2020).

Northern Chad, a confluence point between the central Sahara and the Sahel, represents a highly sensitive climatic transition zone where the balance between water resources and agropastoral activities is precarious (Raimond et al., 2014; Mahamat Nour et al., 2017). Rainfall distribution is strictly governed by the latitudinal position of the Intertropical Front (ITF), the surface expression of the Intertropical Convergence Zone (ITCZ) marking the boundary between the dry harmattan and the moist monsoon (Nicholson, 2013). An anomalous northward migration of the ITF allows for the injection of Atlantic moisture into the heart of the Sahara, triggering deep convection (Sultan and Janicot, 2003; Parker et al., 2005). This dynamics is further modulated by intra-seasonal oscillations (ISO), which influence water vapor transport and moist static energy (MSE) fluxes (Siewe et al., 2025; Wamba et al., 2023) and is often exacerbated by synoptic perturbations, such as African Easterly Waves (AEW) (Kiladis et al., 2006; Lafore et al., 2017).

Beyond dynamics, thermodynamic and radiative factors are decisive. MSE offers a diagnostic framework integrating temperature, humidity, and the vertical structure of the atmosphere (Neelin and Held, 1987; Holloway and Neelin, 2009). High MSE values reduce convective inhibition, facilitating the organization of mesoscale convective systems responsible for extreme accumulations (Romps, 2015). Recent studies demonstrate that these events result from a

6

synergy between thermodynamic instability, radiative flux anomalies, and dynamic forcings such as moist enthalpy advection and potential vorticity anomalies (Kenfack et al., 2024, 2025; Tchana et al., 2025). Simultaneously, vertical velocity characterizes the strength of updraft where negative omega anomalies represent the classic signature of organized convection in West Africa (Taylor et al., 2017; Panthou et al., 2020).

At the global scale, 2024 was characterized by unprecedented warming and a surge in hydrometeorological extremes (Zhang et al., 2025). In August 2024, exceptionally intense rainfall hit the Saharan regions of Chad and the Lake Chad Basin, leading to catastrophic socio-economic impacts, including unusual flooding, infrastructure collapse, agricultural losses, and widespread population displacement (OCHA, 2024). These events revealed the acute vulnerability of regions historically characterized by low rainfall variability. While the 2024 anomaly aligns with a broader Sahelian trend associated with an anomalously northward ITCZ (Zhang et al., 2025; Nicholson, 2013), the specific atmospheric mechanisms driving rainfall in the true Saharan desert remain insufficiently documented. Most existing literature focuses on the Sahelian and Sudanian belts, leaving a gap in our understanding of the joint dynamic and thermodynamic processes, and their socio-economic consequences, within the hyper-arid Sahara and the Lake Chad Basin.

This study aims to fill this gap by characterizing the forcings behind the August 2024 extreme event through an integrated analysis of moisture convergence, remote moisture advection, vertical velocity, and MSE. By linking these physical mechanisms to field observations of socio-economic impacts, this work provides critical insights for climate adaptation and risk management in the Sahara and Lake Chad Basin (Biasutti, 2019; Vizy and Cook, 2022). The article is structured as follows: Section 2 details the study area, the data and methodology; Section 3 presents the dynamic and thermodynamic results; Section 4 discusses the physical mechanisms and associated socio-economic impacts; and Section 5 concludes the study.

2. Study Area, Data and Methods

2.1. Study Area

This study focuses on northern Chad expanding 16°-24°N, 13°-25°E, an area administratively comprising the regions of Tibesti, Borkou, Ennedi West, and Ennedi East (Figure 1). The landscape is dominated by vast sandy plains and longitudinal dune systems. The regional climate is hyper-arid, characterized by extreme thermal amplitudes and negligible annual precipitation. Despite its harsh environment, the Saharan sector of Chad accounts for approximately 13% of the national population (approx. 2.73 million inhabitants; INSEED-Chad). Economic subsistence is primarily linked to oasis-based agriculture, specifically date palm cultivation, and nomadic pastoralism centered on camel herding. The primary urban centers include Faya-Largeau (pop. 100,000), Fada (pop. 50,000), Bardaï (pop 30,000) and Amdjarass

https://doi.org/10.5194/egusphere-2026-725
Preprint. Discussion started: 16 February 2026

(pop. 2,000). These cities, like all inhabited localities, are established in oases to take advantage of the meager water resources available given the hyper-arid environment.

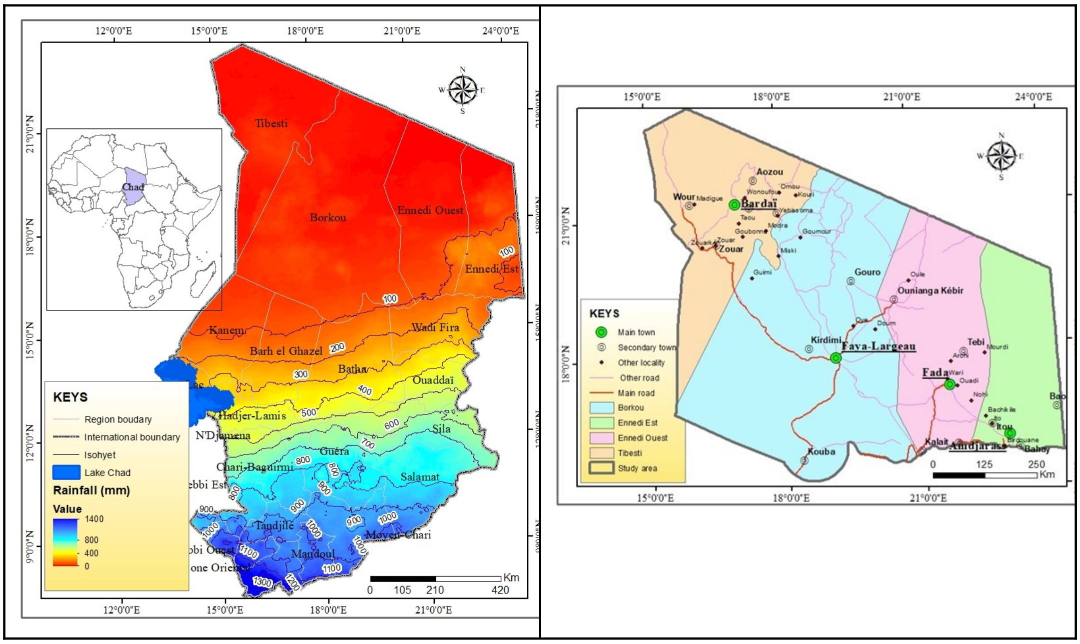

Figure 1. Study area in Chad

2.2. Data

a. Rainfall datasets

The present study employed monthly rainfall data, from the Tropical Applications of Meteorology using SATellite Data v.3.1(TAMSAT) rainfall estimate (Maidment et al., 2017) and Climate Hazards Group InfraRed Precipitation with Station data (CHIRPS) (Funck et al., 2015), spanning from 1983 to 2024. The aim is to analyze, in the two datasets, the interannual variations and thrend of the August rainfall.

CHIRPS is a global precipitation dataset comprising data from over 30 years. The integration of satellite imagery at a 0.05°x0.05° resolution with in-situ station data enables the generation of gridded precipitation time series, facilitating the analysis of trends and the monitoring of seasonal droughts. The CHIRPS dataset used is publicly accessible for download (https://www.chc.ucsb.edu/data/chirps3). TAMSAT estimates are derived from a synergy of Meteosat Thermal Infrared (TIR) imagery and ground-based rain gauge calibrations (Maidment et al., 2017). The algorithm utilizes Cold Cloud Duration (CCD) to estimate rainfall, a method particularly effective for convective systems in Africa (Wainwright et al., 2021). The data feature

https://doi.org/10.5194/egusphere-2026-725
Preprint. Discussion started: 16 February 2026

11

a high spatial resolution of 0.0375° (~4 km), facilitating a detailed characterization of rainfall distribution across the complex Saharan topography.

b. The ERA5 reanalysis

Atmospheric conditions were analyzed using the ERA5 reanalysis, the fifth-generation global climate dataset produced by the European Centre for Medium-Range Weather Forecasts (ECMWF) (Hersbach et al., 2020). ERA5 offers significant advancements over its predecessor, ERA-Interim, including enhanced spatial and temporal resolutions and a more sophisticated data assimilation system. These improvements allow for a more physically consistent representation of the hydrological cycle and atmospheric dynamics over the African continent.

Previous evaluations have demonstrated that ERA5 accurately captures rainfall variability, moisture transport, and large-scale circulation patterns over equatorial and Sahelian Africa (Johannsen et al., 2019; Cook and Vizy, 2021). Furthermore, the dataset's internal consistency between dynamic and thermodynamic variables makes it a robust tool for diagnosing extreme hydroclimatic events in data-sparse regions like the Sahara (Tarek et al., 2020; Ssenyunzi et al., 2020). The dataset features a 0.25° × 0.25° horizontal resolution and a vertical discretization of 137 pressure levels (surface to 0.01 hPa). For this study, we extracted monthly fields of horizontal and vertical wind components, geopotential height, specific humidity, temperature, and vertical velocity (ω). The analysis focuses on the month of August for the 1983-2024 period, coinciding with the peak of the West African Monsoon's northward migration. This timeframe provides a stable climatological baseline to evaluate the mechanisms driving the exceptional anomalies observed in northern Chad during 2024.

c. Data on flood losses

Due to Chad's fragile socioeconomic and security context, systematic disaster recording is primarily facilitated by international humanitarian organizations and United Nations agencies in collaboration with the Chadian government. For the 2024 flood event, impact data were obtained from the United Nations Office for the Coordination of Humanitarian Affairs (OCHA), which synthesizes inter-agency field reports. These data are validated by the Ministry of Territorial Administration and Decentralization, alongside the Ministry of Social Action, Solidarity, and Humanitarian Affairs.

The dataset includes standardized metrics on:

- Human casualties (mortality and injury rates);
- Displaced populations and affected households;
- Agricultural losses (hectares of devastated cropland);
- Infrastructure damage (destruction of homes and commercial facilities);
- Livestock mortality.

12

https://doi.org/10.5194/egusphere-2026-725
Preprint. Discussion started: 16 February 2026

While national summaries typically emphasize the southern and central provinces due to their higher absolute population densities (e.g., Mayo-Kebbi Est, Lac, and Tandjilé), this study specifically isolates data for the northern Saharan provinces. Although the absolute number of victims in these arid regions is lower compared to the south, the relative impact, defined as the ratio of affected individuals to the total provincial population, is among the highest recorded in 2024. This relative approach is essential for assessing the exceptional nature of climate extremes in sparsely populated hyper-arid zones. Data was accessed via the OCHA Chad humanitarian portal (https://www.unocha.org/chad).

2.3. Methods

To diagnose the physical mechanisms driving the exceptional rainfall of August 2024, a suite of diagnostic variables was employed. The methodological framework distinguishes between thermodynamic precursors (the energy and moisture required for convection) and dynamic forcing (the atmospheric mechanisms triggering vertical motion).

a. Climatological Anomaly Calculation

The primary method for quantifying the departure of the 2024 event from historical norms is the calculation of climatological anomalies. For a given variable , the August 2024 anomaly (X'_{2024}) is defined as the difference between the observed monthly value (X_{2024}) and the long-term climatological mean (X) calculated over the 1983-2023 reference period:

$$X'_{2024} = X_{2024} - \frac{1}{n}\sum_{i=1983}^{2023} X_i$$

where $n=41$ years. Positive anomalies signify values exceeding the historical baseline, while negative anomalies denote deficits.

b. Detection of the Intertropical Front (ITF)

The ITF serves as a critical diagnostic for monitoring the northward penetration of the West African Monsoon (WAM) into the Saharan heat low. In this study, the latitudinal position of the ITF is identified using the 15°C isodrosotherm (dew point temperature $T_d=15°$) at the 925 hPa level, following the criteria established by Nicholson (2013). This boundary marks the interface between the moist south-westerly monsoon flow and the dry north-easterly Harmattan.

c. Wind Convergence Analysis

To identify zones of mechanical forcing, we analyze horizontal wind convergence at the 850 hPa level. Low-level convergence is the primary driver for mass inflow that sustains vertical updrafts. The horizontal divergence (D) is calculated as:

$$D = \nabla . V = \frac{\partial u}{\partial x} + \frac{\partial v}{\partial y}$$

https://doi.org/10.5194/egusphere-2026-725
Preprint. Discussion started: 16 February 2026

Where and are the zonal and meridional wind components, respectively. A negative value of *D* (*D*< 0) represents convergence, indicating a mass inflow that sustains vertical updrafts.

d. Moist Static Energy (MSE) and Moisture Flux Convergence

Moist Static Energy (MSE) is used to evaluate the convective potential and stability of the atmosphere (Neelin and Held, 1987; Kenfack et al., 2025). It integrates sensible heat, potential energy, and latent heat:

$$MSE = C_p T + gz + L_v q$$

Where:

C_p is the specific heat of dry air at constant pressure (1004 J.Kg-1.K-1); T is the absolute temperature (K), g is the gravitational acceleration (9.81 m.s-1), L_v is the latent heat of vaporization, z is the geopotential height (m), and q is the specific humidity (Kg.Kg-1). By examining MSE anomalies, we can establish if the August 2024 extremes were driven by an unusual amount of moisture (latent heat) or intense localised surface heating (sensible heat).

2.5 Vertical Velocity (ω)

We also explored the intensity of the atmospheric ascent triggered by the convergence by analyzing the vertical velocity in pressure coordinates (ω). Significant negative values (ω < 0) indicate strong upward motion throughout the tropospheric column, which is the dynamic signature of deep convective cells (Taylor et al., 2017; Tchana et al., 2025).

3. Results

3. 1 The record-breaking August 2024 rainfall in the Chadian Sahara

The interannual variation in August rainfall in northern Chad (16°-24°N, 13°-25°E) characterizes a hydro-climatic regime defined by extreme scarcity and structural volatility, where monthly totals historically hover around a low climatological base of 9 to 13 mm. This dynamic is intrinsically linked to the Saharo-Sahelian transition zone, where rainfall depends strictly on erratic excursions northward of the Intertropical Convergence Zone (ITCZ) and the associated dynamics of the African East Jet (AEJ) (Nicholson et al., 2013; 2018). Analysis of time series over the period 1983-2024, comparing TAMSAT and CHIRPS satellite products (Fig. 2), reveals

https://doi.org/10.5194/egusphere-2026-725
Preprint. Discussion started: 16 February 2026

remarkable consistency in capturing phases of variability, accurately identifying drought cycles (1984, 1990, 2000) and wetter episodes (1999, 2018-2020). Although a systematic bias appears between the two algorithms, with TAMSAT showing an average of 12.7mm compared to 9.6 mm for CHIRPS, the overall climate trajectory is unambiguous. There is a clear transition from a phase of persistent drought in the 1980s to a robust and statistically significant upward trend, as evidenced by the extremely low p-values (1.35×10^{-5} for TAMSAT and 1.06×10^{-4} for CHIRPS). A major visual indicator of this change is the intersection point between the trend line and the climatological average, located around the year 2003. This intersection is a true statistical turning point: it marks the moment when the region's “new normal” exceeded the historical average for the period 1983-2024. Before this point, the signal was weighted by the extreme aridity of decades of drought; after 2003, the trend line rising above the average indicates that the rainfall regime has entered a phase of structural excess compared to the past. In terms of decadal variability, this shift is reflected in a clear intensification: while the period 1993-2012 showed a simple return to equilibrium, the decade after 2013 (and particularly after 2017) has been marked by increasingly frequent and closely spaced peaks, suggesting that the region is moving away from its traditional hyper-arid state towards a more unstable and humid climate.

https://doi.org/10.5194/egusphere-2026-725
Preprint. Discussion started: 16 February 2026

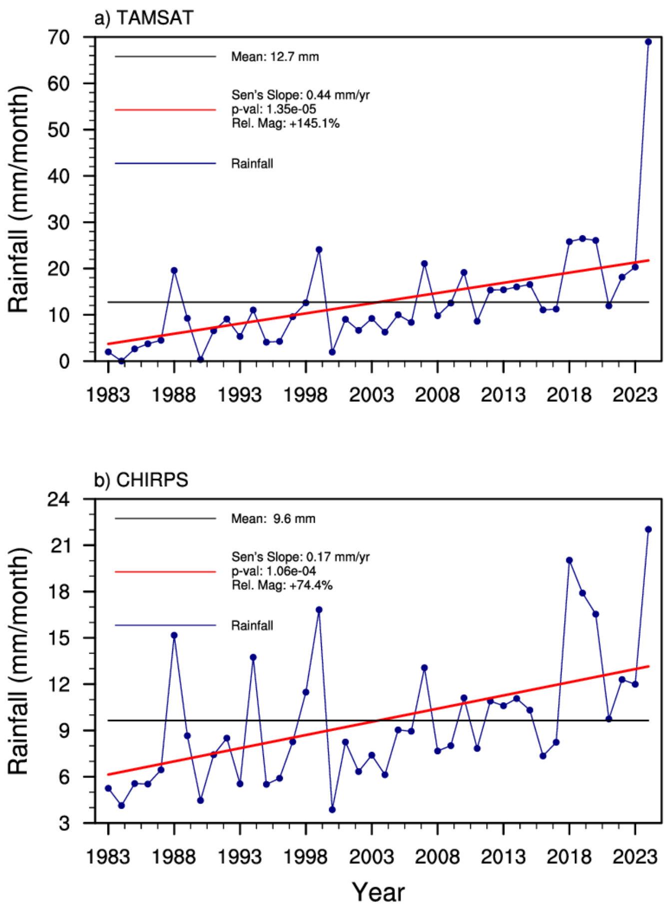

Figure 2: Precipitation trends and patterns in the 16°-24°N / 13°-25°E region in August (1983-2024). A comparison of TAMSAT (a) and CHIRPS (b) satellite data is shown. The red line shows the trend line; the black line shows the average over the study period.

This change is reflected in a positive Sen slope (0.44 mm/year for TAMSAT) and a massive relative magnitude of up to +145%, confirming a profound change in the water regime that goes beyond simplerandom variability and is part of the "greening" signal in the Sahel (Brandt et al., 2015). The record anomaly in August 2024, when precipitation exceeded the exceptional threshold of 70 mm/month, marked the culmination of this intensification. Such an event, exceeding the historical average by more than four to five standard deviations, reflects an unprecedented northward penetration of the WAM, illustrating how current thermodynamic forcings amplify the magnitude of extreme hydrological events in traditionally hyperarid regions of the Sahara. These developments have major hydrological implications for the entire Lake Chad basin. Although the north is located outside the active runoff production zone, the increase in rainfall after the 2003 pivot point is changing the regional water balance. Such intensification contributes to the recharge of shallow aquifers and the reactivation of fossil wadis. For Lake Chad, this means a slowdown in evaporation and increased surface inflow from its

https://doi.org/10.5194/egusphere-2026-725
Preprint. Discussion started: 16 February 2026

northern margins, although this dynamic also exposes pastoral areas to unprecedented risks of flash flooding.

3.2. Atmospheric drivers

3.2.1. Climatological mean position and anomalies of the Intertropical Front (ITF) at 850 hPa

Figure 3 displays the spatial distribution of 850 hPa wind convergence, horizontal wind vectors, and the latitudinal position of the ITF, defined by the 15°C dew point isodrosotherm. Three states are compared: the 1983-2023 August climatology (Fig. 3a), the August 2024 observed state (Fig. 3b), and the resultant anomalies (Fig. 3c).

In the climatological mean (Fig. 3a), the ITF is typically positioned between 15°N and 18°N. Significant low-level convergence is confined to the Sahelian belt, driven by the moisture-laden southwesterly monsoon flow. Conversely, Northern Chad is dominated by a divergent regime associated with the subsiding branch of the Hadley cell and dry northeasterly Harmattan winds, conditions that inhibit deep convection. This configuration is consistent with the established structure of the WAM, where low-level convergence is the primary trigger for convective activity (Sultan & Janicot, 2003; Nicholson, 2013). In August 2024 (Fig. 3b), the atmospheric circulation underwent a radical shift. The ITF exhibited an anomalous northward migration, reaching 20°N-22°N. This displacement facilitated the deep penetration of southwesterly monsoon surges into the Saharan interior. Consequently, the core of low-level convergence shifted significantly northward, establishing the dynamic engine necessary for sustained vertical motion in regions that are climatologically stable. Similar mechanisms involving anomalous southwesterly moisture intrusions and strong low-level moisture flux convergence have been shown to underpin extreme multi-day rainfall events in northern tropical Africa, particularly when such flows reinforce a northward-displaced ITF and interact with regional-scale circulation anomalies (Vondou et al., 2025).

The wind field analysis reveals a low-tropospheric cyclonic anomaly centered between 15°N and 20°N. This feature not only enhanced horizontal convergence but also increased cyclonic vorticity, which is essential for the organization and longevity of Mesoscale Convective Systems (MCSs) (Lavaysse et al., 2009; Flamant et al., 2018).

The anomaly field (Fig. 3c) confirms that the 2024 convergence patterns were statistically significant at the 95% confidence level (exceeding two standard deviations). These positive convergence anomalies are spatially in-phase with the northward wind anomalies, signalling a total disruption of the typical Saharan divergent regime. This transition represents a temporary northward expansion of the Sahelian convective climate into the hyper-arid Saharan zone (Taylor et al., 2017; Biasutti, 2019). Broadly, the extreme rainfall of August 2024 resulted from a synergistic interaction between the exceptional northward migration of the ITF, a reinforced low-level convergence at 850 hPa and the establishment of a regional cyclonic circulation that sustained the ascent of warm, moist air masses. These findings align with recent literature linking increased WAM variability to higher frequencies of hydroclimatic extremes in the Sahara-Sahel transition zone (Taylor et al., 2017; Biasutti, 2019; Janicot et al., 2008; Panthou et al., 2020).

https://doi.org/10.5194/egusphere-2026-725
Preprint. Discussion started: 16 February 2026

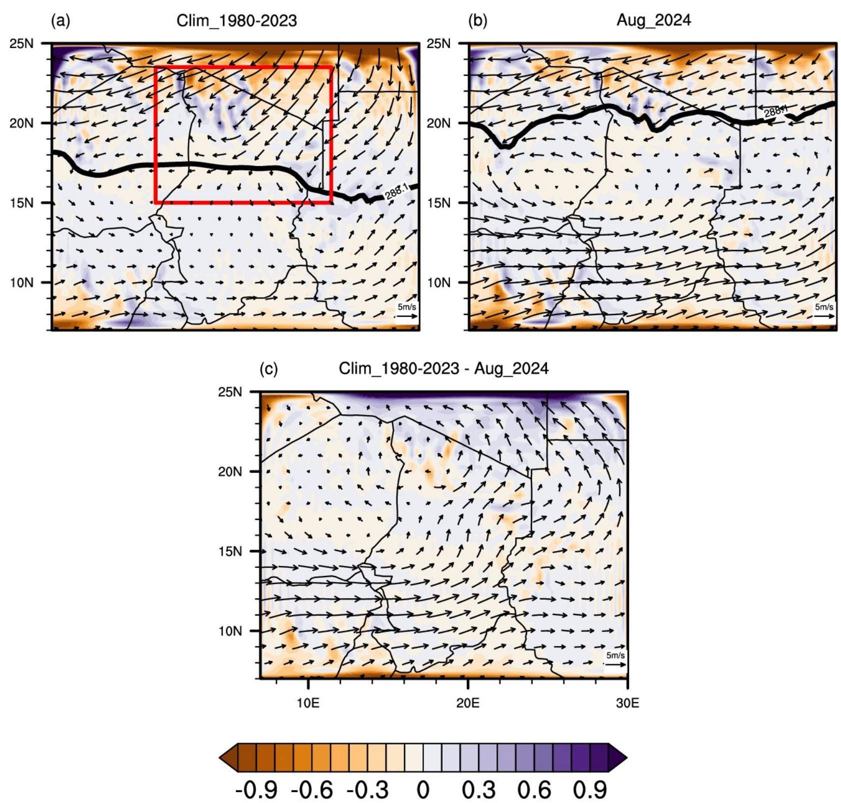

Figure 3. Spatial distribution of lower-tropospheric wind convergence at 850 hPa (shaded; s^{-1}), horizontal wind vectors ($m\ s^{-1}$), and the mean position of the Intertropical Front (ITF; solid black contour), defined by the 15°C dew point isodrosotherm. The panels represent: (a) the August climatology (1983-2023), (b) the observed conditions in August 2024, and (c) the 2024 anomalies (relative to the 1983-2023 baseline). The reference vector represents a wind speed of 5m s^{-1}. The red box delimits the study domain (Northern Chad; 16N-24N, 13E-25E)

3.2.2. Composite anomalies of wind and humidity (850 hPa)

Figure 4 displays the spatial distribution of specific humidity at 850 hPa (shaded) superimposed with horizontal wind vectors at the same level over Central and Saharan Africa. Three configurations are analyzed: (a) the August climatology for the 1980-2023 period, (b) the conditions observed in August 2024, and (c) the anomalies, defined as the difference between August 2024 and the climatological mean.

The climatology (Fig. 4a) reveals a pronounced meridional gradient of specific humidity, with high values confined south of approximately 15°N-18°N, corresponding to the mean northernmost extent of the West African Monsoon (WAM). Low-tropospheric winds are dominated by a southwesterly flow south of the Intertropical Front (ITF), ensuring the advection of moist air toward the Sahelian belt. In contrast, the northern Saharan regions remain under the

https://doi.org/10.5194/egusphere-2026-725
Preprint. Discussion started: 16 February 2026

influence of much drier air and weak zonal circulation, conditions generally unfavorable for convective activity. This configuration reflects the mean monsoon regime, where the distribution of low-level moisture acts as a primary control on summer convection (Nicholson, 2013; Biasutti, 2019).

In August 2024 (Fig. 4b), the specific humidity structure deviated markedly from the climatological mean. Enhanced humidity values extended anomalously northward, locally reaching 20°N-22°N, indicating an exceptional penetration of moist monsoonal air into the Saharan region. This northward extension was coupled with strengthened low-level winds, which facilitated efficient moisture advection from the Gulf of Guinea toward the Central Sahel and Sahara. These features reflect both an intensification and a northward expansion of the low-level moisture pool, serving as a critical precondition for the development of extreme precipitation events over typically arid regions.

The anomaly field (Fig. 4c) highlights strong positive specific humidity anomalies at 850 hPa over large portions of the Saharan domain, in phase with wind anomalies that favored meridional moisture transport. These anomalies suggest a clear breakdown of the climatological regime, which is typically characterized by a low-level moisture deficit north of the Sahel. They confirm the establishment of an exceptionally favorable thermodynamic environment for deep convection, consistent with the observed northward shift of the monsoon in August 2024.

Combined with the previously identified positive anomalies of low-level convergence at 850 hPa, these moisture surpluses point to a particularly effective dynamical-thermodynamical coupling. Low-level convergence enhances upward motion, while abundant near-surface moisture reduces convective inhibition and promotes the development of organized mesoscale convective systems (MCSs), the primary contributors to extreme rainfall over West Africa.

Overall, Figure 4 demonstrates that the extreme rainfall observed in August 2024 over Saharan regions did not result solely from favorable dynamical forcing, but also from a major anomaly in low-level moisture content associated with an exceptional northward shift of the West African Monsoon.

https://doi.org/10.5194/egusphere-2026-725
Preprint. Discussion started: 16 February 2026

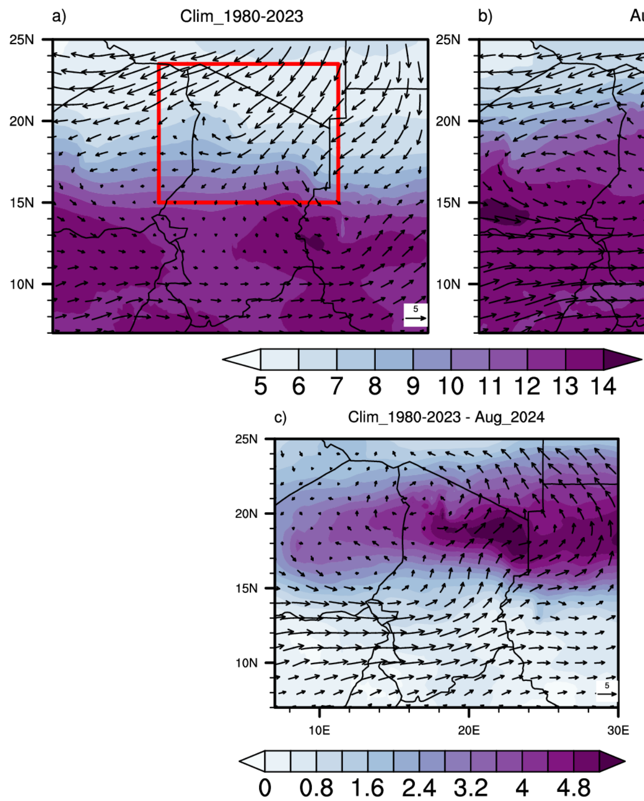

Figure 4: Spatial distribution of specific humidity and wind fields at 850 hPa in August. The red box delimits the study domain (Northern Chad; 15N-24N, 13E-25E). Panels represent: (a) the 1980-2023 climatological mean; (b) August 2024 conditions; and (c) August 2024 anomalies relative to the climatology, showing specific humidity (kg.kg^{-1}, shaded) and wind vectors. Only anomalies exceeding two standard deviations are shown. A 5 m/s reference wind vector is displayed in the bottom right corner of each panel.

3.2.3. Latitude-pressure cross-sections of vertical velocity

Figure 5 presents the latitude-pressure cross-sections of vertical velocity (ω, 10^{-2} x Pa.s^{-1}, shaded) for August, averaged over the longitudinal band 13°E-24°E. The overlaid vectors, constructed from the meridional wind component (v) and vertical velocity (ω), illustrate the structure of the meridional-vertical circulation (Hadley-type cell). Three configurations are analyzed: (a) the August climatology for the 1980-2023 period, (b) the conditions observed in August 2024, and (c) the anomalies, defined as the difference between August 2024 and the climatological mean. Following the ERA5 convention, negative ω values (blue shading) indicate upward motion, while positive values (red shading) correspond to subsidence.

https://doi.org/10.5194/egusphere-2026-725
Preprint. Discussion started: 16 February 2026

In climatology (Fig. 5a), the mean circulation is characterized by a well-defined ascending branch (ω < 0) centered between approximately 10°N and 15°N, extending from the lower troposphere (850-700 hPa) into the upper troposphere (up to 300 hPa). This deep ascent corresponds to the Sahelian convective zone associated with the WAM. North of about 18°N-20°N, the circulation is dominated by subsiding motions, particularly above 600 hPa, reflecting the influence of the dry Saharan regime and the descending branch of the Hadley cell. Within the study region (16°N-24°N), ascending motions remain shallow and largely restricted to the lower and mid-troposphere, where they are rapidly capped by subsidence aloft. This vertical structure is consistent with the climatological southward position of the ITF and with a low-level convergence regime primarily confined to the Sahel, as indicated by the 850 hPa circulation. The vectors illustrate a coherent but latitudinally limited overturning cell, with low-level inflow and upper-level outflow concentrated south of the Sahara.

In August 2024 (Fig. 5b), the meridional circulation underwent a marked reorganization. Intense ascending motions extended anomalously far north, reaching approximately 18°N-22°N, and exhibited substantially increased vertical depth. This change is directly linked to the exceptional northward displacement of the ITF, which brought the core of low-level convergence at 850 hPa into the Saharan interior. The resulting sustained inflow of warm and moisture-laden air in the lower troposphere fueled persistent ascent throughout the atmospheric column, as evidenced by the dominance of negative ω values from the surface up to ~200 hPa. Simultaneously, the meridional overturning circulation intensified, indicating enhanced poleward transport of moisture and energy toward Saharan latitudes. Such a configuration is dynamically highly favorable to the development and maintenance of organized deep convection, representing a clear departure from the climatological Saharan regime.

The anomaly field (Fig. 5c) highlights pronounced negative ω anomalies over a broad latitudinal band extending from approximately 16°N to 24°N, with maximum amplitude in the lower and middle troposphere (850–500 hPa). This pattern marks a clear departure from the climatological Saharan regime, where subsidence typically prevails north of the Sahel, and indicates a significant northward displacement of the ascending branch of the West African Monsoon. The associated meridional wind anomalies reveal a strengthened overturning circulation that favors sustained ascent over normally arid regions. Together, these anomalies reflect a deep destabilization of the atmospheric column, providing a dynamical explanation for the persistence and intensity of the exceptional rainfall observed in August 2024.

In general, these results indicate that in August 2024, the atmospheric circulation was characterized by an unusual intensification and northward expansion of the ascending branch of the WAM. This is consistent with the previously identified anomalies in lower-tropospheric convergence and moisture. The presence of deep, persistent, and spatially extensive ascent represents a key mechanism explaining the extreme rainfall observed over Saharan regions, as it facilitates the development and organization of intense Mesoscale Convective Systems

https://doi.org/10.5194/egusphere-2026-725
Preprint. Discussion started: 16 February 2026

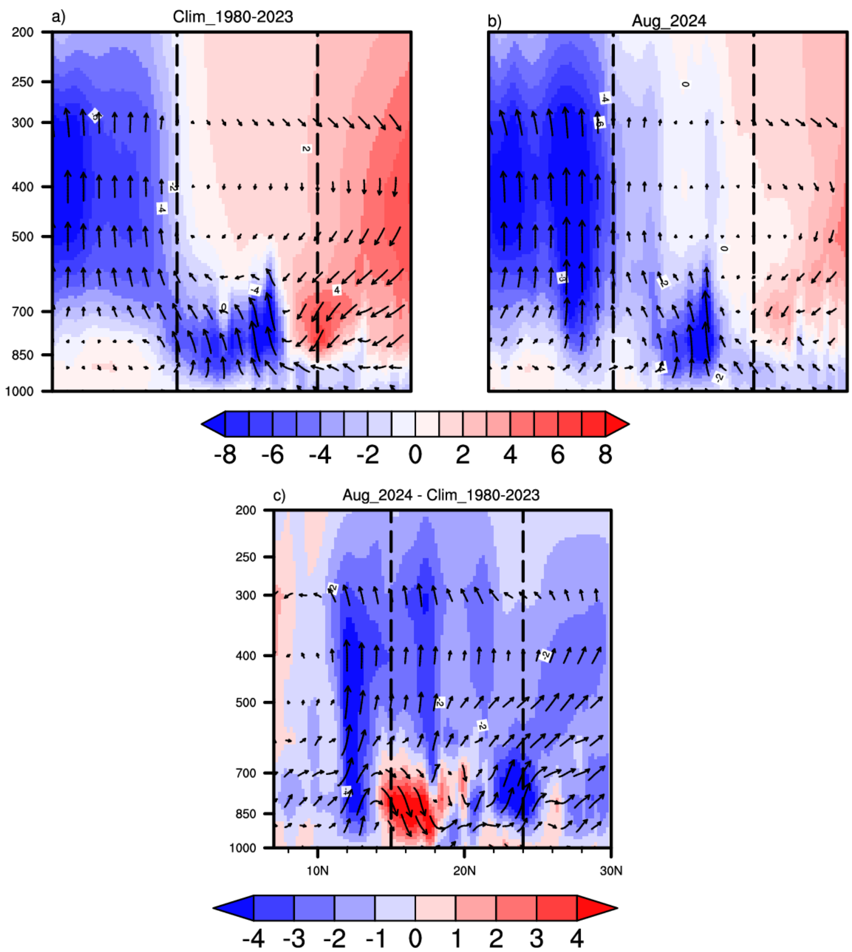

Figure 5: Latitude-pressure cross-sections of vertical velocity (ω, ×10−2 Pa.s^{-1}, shaded) and zonal-vertical circulation (v, vectors) in August. Vertical velocity is averaged over the longitudinal band 13°E-25°E. The vertical dotted lines delimit the latitudinal band of our study area. The overlaid vectors represent the combined zonal and vertical circulation (v and ω). Panels show (a) the 1980 - 2023 climatology, (b) August 2024, and (c) anomalies calculated as the difference between August 2024 and the climatological mean. Negative ω values indicate upward, whereas positive values correspond to subsidence motion.

3.2.4. Spatial patterns of moist static energy anomalies

Figure 6 illustrates the spatial anomalies of moist static energy (MSE; shaded, kJ kg^{-1}) and contours of equivalent potential temperature (θe; red, K) over the Sahelian and Saharan regions. As an integrative variable combining thermal, gravitational, and latent energy contributions,

https://doi.org/10.5194/egusphere-2026-725
Preprint. Discussion started: 16 February 2026

MSE provides a robust diagnostic for linking dynamic forcing (convergence and ascent) to the thermodynamic conditions conducive to deep convection (Neelin and Held, 1987; Romps, 2015). Positive MSE anomalies dominate the central and eastern Sahara, with maxima reaching 10-12 kJ kg^{-1} north of the Sahel, centered between 18°N and 25°N. This structure reflects an anomalous energetic enrichment of the lower and middle troposphere in regions typically characterized by low energy content and strong convective inhibition (CIN). Conversely, regions farther south exhibit weaker MSE anomalies, suggesting a northward displacement of the monsoon-related energy reservoir. Horizontal convergence at 850 hPa acts as a dynamic pump, driving the ascent of warm, moist air and enhancing MSE in the mid-troposphere (Raymond et al., 2009). This low-level forcing propagates vertically, as evidenced by negative ω anomalies (enhanced ascent) between 850 and 300 hPa. The spatial colocation of MSE maxima, convergence zones, and ascent cores suggests a dynamic-thermodynamic locking mechanism, wherein increased MSE reduces CIN while persistent ascent sustains the organization and longevity of deep convection.

Contours of θe show a structure consistent with MSE anomalies. The tightening and deformation of contours near MSE maxima indicate enhanced horizontal gradients, reflecting interactions between low-level warm advection and diabatic heating from convective activity. The coincidence of strong MSE anomalies and elevated θe suggests that the MSE increase stems from the combined effects of enhanced moisture advection and local tropospheric warming. This is consistent with theoretical frameworks linking the vertical structure of MSE to convective stability and energy conversion efficiency in the tropics (Romps, 2015; Holloway and Neelin, 2009).

This MSE-θe coupling highlights a profound reorganization of the regional thermodynamic environment. Persistent positive MSE anomalies are known precursors to extreme rainfall in West Africa when spatially coherent with lower-tropospheric dynamic forcing (Taylor et al., 2017). The observed configuration aligns with an anomalous northward extension of the Sahelian convective regime, corresponding to the northward displacement of the Intertropical Front (ITF).

In a broader context, these anomalies are consistent with mechanisms linking West African monsoon intensification to increased frequency and intensity of extreme rainfall over the Sahara (Biasutti, 2019; Vizy and Cook, 2022). The joint analysis of MSE, lower-tropospheric convergence, and vertical velocity (ω) underscores an integrated mechanism: convergence strengthens ascent, which promotes the vertical homogenization of MSE; in turn, elevated MSE sustains intense, long-lasting deep convection. This positive dynamic-thermodynamic feedback is a key driver behind the magnitude of the extreme rainfall observed in August 2024.

https://doi.org/10.5194/egusphere-2026-725
Preprint. Discussion started: 16 February 2026

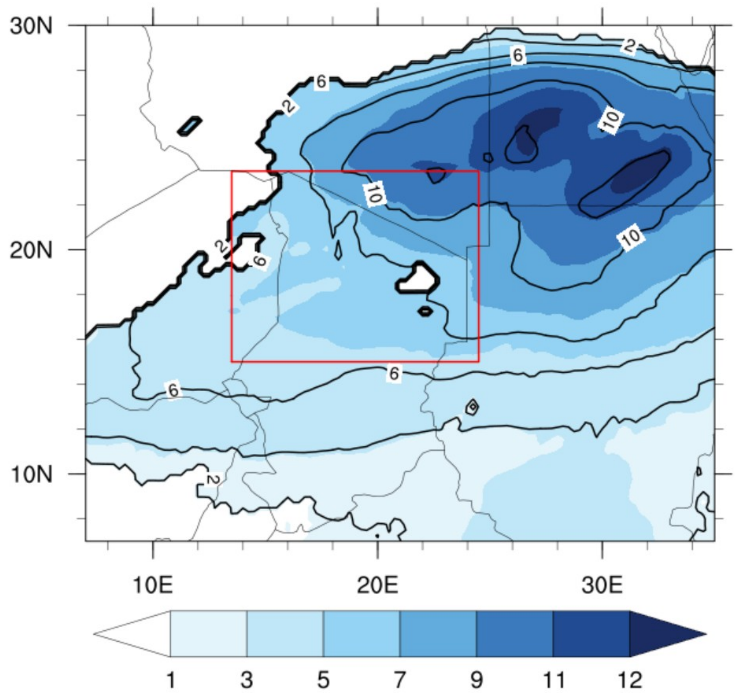

Figure 6. Spatial anomalies of moist static energy (MSE; shaded, kJ kg^{-1}) and equivalent potential temperature (θe; black contours, K). The map illustrates the coupling between regional thermodynamic variability and the spatial organization of MSE over the Sahel-Saharan region. The superposition of these fields highlights the northward expansion of high-energy air masses and the intensification of the monsoon-related energy reservoir.

3.2.5. Contribution of August 2024 rainfall to the climatological mean

Figure 7 illustrates the exceptional nature of the August 2024 rainfall anomalies across the study region. Compared to the long-term August climatology (Fig. 7a), the August 2024 period exhibits a significant intensification of precipitation, particularly across the eastern sector (Fig. 7b). The relative contribution map (Fig. 7c) reveals localized positive anomalies exceeding 80-100%, indicating that the rainfall during this single month nearly doubled the historical average in several areas.

This spatial pattern is consistent with an anomalous northward displacement of the ITF, which facilitated the deep penetration of monsoon moisture into typically arid Saharan latitudes. This increased moisture availability preconditioned the lower troposphere, enhancing its sensitivity to dynamical triggers. Consequently, the regions with the highest contribution rates align with areas of intensified low-level convergence, likely modulated by the passage of an AEW. The synergy

https://doi.org/10.5194/egusphere-2026-725
Preprint. Discussion started: 16 February 2026

between an intensified monsoon flux, a northward-shifted ITF, and AEW-driven ascent accounts for the localized extremes observed in August 2024.

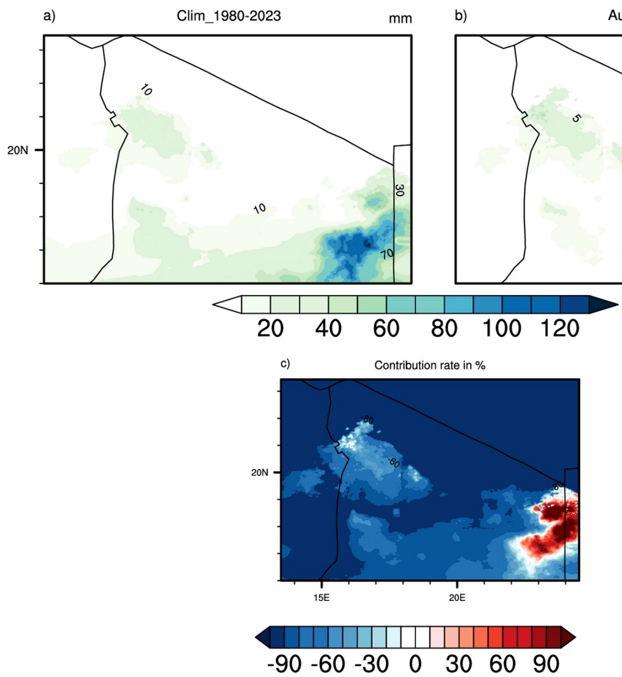

Figure 7: Spatial distribution of August rainfall and relative contribution of the 2024 event. (a) August rainfall climatology for 1980-2023, (b) observed August 2024 rainfall, and (c) relative contribution (%) of the August 2024 rainfall with respect to the climatology.

The spatial distribution of these rainfall anomalies (Fig. 7) is closely coupled with coherent features in the lower- and mid-tropospheric fields. The precipitation maxima and peak contribution rates are collocated with enhanced 850 hPa wind convergence, meaning a strengthened monsoon inflow and moisture pooling south of the displaced ITF. This convergence is supported by positive specific humidity anomalies and elevated moist static energy (MSE), reflecting a deepened moist layer and reduced convective inhibition.

Consistent with these findings, the affected regions exhibit pronounced negative ω anomalies, confirming enhanced large-scale ascent. The spatial synchronization of vertical motion, moisture convergence, and MSE maxima underscores the critical role of vertical coupling in sustaining organized deep convection. By allowing the meridional transport of moisture into the Sahara, the ITF shift created a favorable thermodynamic environment, while synoptic-scale disturbances from AEWs provided the necessary dynamical forcing to trigger and maintain the observed extreme precipitation events.

3.3. Socio-economic impacts of the August 2024 extreme event

In 2024, Chad experienced the most catastrophic flooding in its recorded history. Nationwide, the impact was profound: nearly 2 million people were affected, resulting in 576 confirmed fatalities. The floods submerged approximately 432,800 hectares of agricultural land, destroyed 217,700 homes, and led to the loss of 72,100 head of livestock. Furthermore, infrastructure damage was extensive, with 3,058 schools severely impacted. Geographically, the crisis was universal, affecting all 23 provinces. Notably, the Saharan provinces, typically spared due to their hyper-arid climate, suffered disproportionately heavy losses.

In the desert zone, initial warnings were issued in July as flooding began in the south. However, torrential rains struck the northern desert region with unprecedented intensity between August 9th and 14th, 2024. National meteorological records documented 126.5 mm of rainfall over eight days in areas where total annual precipitation rarely reaches 100 mm. These levels represent the highest rainfall totals in 60 years. Visual evidence (Fig. 8) corroborates these records, showing water levels reaching knee-depth at the Faya-Largeau market, where commercial and material losses were severe.

Figure 8: Flooded streets and commercial stalls at the Faya-Largeau market (Source: Tchad Info Société).

Within the specific study area, the flooding impacts are categorized by human displacement, mortality, agricultural devastation, and infrastructural loss. While national reports often aggregate these figures, detailed provincial data is typically only prioritized where significant loss of life occurs. Consequently, the situations in Borkou (4 deaths) and Tibesti (60 deaths) are better documented than in the Ennedi provinces, which reported no fatalities. However, OCHA situational reporting as of October 1, 2024, allows for a more granular assessment of the affected populations across all study provinces. This disparity highlights the critical need for developing nations to enhance civil protection services and systematic data collection during hydrometeorological disasters (Saha et al., 2018; Mazhin et al., 2021).Table 1 presents the damage breakdown for each province covered by this study.

Table 1: Losses due to flooding in the study provinces

Region	Number of families affected	Number of people affected	Number of dead recorded	Number of houses/ shops destroyed	number of aminal kill
Borkou	10 402	67 613	04	23 174 houses	861
Ennedi East	35 980	233 872			
Ennedi West	1 842	11 977			
Tibesti	23	150	60	Thousands shops	

Beyond the quantified losses in Table 1, the regional economy, heavily reliant on trade and mining, suffered significant shocks. Thousands of shops were destroyed, and merchandise was lost. In the Tibesti region, gold mining operations suffered immense equipment losses. A particularly grave secondary hazard emerged as the 2024 floods unearthed thousands of landmines remaining from previous conflicts, creating a long-term security and humanitarian risk for the local population.

Conclusion

This study elucidates the multi-scale atmospheric mechanisms that drive the unprecedented rainfall observed in August 2024 across the Saharan region. Through an integrated analysis of lower-tropospheric convergence, specific humidity, ω, and moist static energy (MSE), the results demonstrate that August 2024 deviated significantly from historical climatology. This anomaly was primarily driven by an exceptional northward migration of the ITF, which reached latitudes of 20-22°N, supported by a synchronized intensification of the WAM.
The northward shift was characterized by significant positive 850 hPa convergence anomalies, a sharp increase in lower-tropospheric specific humidity, and the meridional extension of the upward branch of the Hadley-type circulation. This is evidenced by pronounced negative ω anomalies extending from the lower to the mid-troposphere. Concurrently, substantial positive MSE anomalies over the Sahara indicate a profound thermodynamic enrichment of the

https://doi.org/10.5194/egusphere-2026-725
Preprint. Discussion started: 16 February 2026

atmospheric column in regions typically dominated by large-scale subsidence and moisture deficits.

The synthesis of these variables reveals a coherent dynamic-thermodynamic coupling: lower-tropospheric convergence facilitated the forced ascent and advection of warm, moist air, which in turn promoted the vertical homogenization of MSE. This high-energy environment provided the necessary instability to sustain the development and organization of mesoscale convective systems (MCSs), resulting in the exceptional rainfall totals observed. The socio-economic consequences of this event were devastating, ranging from substantial loss of life to the large-scale destruction of private property and public infrastructure. The scale of this disaster underscores the extreme vulnerability of hyper-arid regions to hydrological hazards. Furthermore, the observed intensification of the hydrological cycle suggests that such events may increase in frequency; consequently, there is an urgent need for regional authorities to transition from reactive disaster management to proactive climate adaptation strategies.

These findings align with recent literature linking WAM variability to intensifying rainfall extremes in West Africa. By emphasizing the synergy between dynamic forcing and thermodynamic preconditioning, this study provides critical insights for improving the representation of Saharan convective extremes in climate models and assessing their future evolution within the context of global climate change.

CODE AVAILABILITY

Figures shown in this study are plotted using the NCAR Command Language (NCL; https://doi.org/10.5065/D6WD3XH5, NCAR Command Language, 2017) and QGIS. Codes can be obtained from the corresponding author.

DATA AVAILABILITY STATEMENT

The ERA5 data were obtained from the Copernicus Climate Change Service (C3S) Climate Data Store (https://cds.climate.copernicus.eu). Climate Hazards Group InfraRed Precipitation with Station data (CHIRPS) is available through the link https://www.chc.ucsb.edu/data/chirps3
The TAMSAT rainfall estimates and derived products are based on Meteosat thermal infra-red (TIR) imagery provided by EUMETSAT (https://data.tamsat.org.uk/data-download/rainfall/)

AUTHOR CONTRIBUTIONS

CWT: conceptualization; data analysis; formal analysis; investigation; methodology; writing original draft; writing ; review and editing. FS: supervision; conceptualization; data analysis ; investigation; validation ; writing original draft ; review and editing. ATT: conceptualization; investigation; methodology; project administration; resources; supervision; validation; writing ; review and editing.

COMPETING INTERESTS

The authors declared that they have no conflict of interests.

ACKNOWLEDGEMENTS

The authors thank all the observational and reanalysis data providers used in this study and the research of the International Joint Laboratory "Dynamics of Terrestrial Ecosystems in Central Africa: A Context of Global Changes" (IJL DYCOCA/LMI DYCOFAC).

The authors acknowledge the use of Gemini AI (Google) for linguistic refinement and stylistic editing of the manuscript

References

Adeyeri, O. E. (2025). Hydrology and climate change in Africa: Contemporary challenges, and future resilience pathways. *Water*, *17*(15), 2247. https://doi.org/10.3390/w17152247

Adeyeri, O. E., Lawin, A. E., Laux, P., Ishola, K. A., & Ige, S. O. (2019). Analysis of climate extreme indices over the Komadugu-Yobe basin, Lake Chad region: Past and future occurrences. *Weather and Climate Extremes*, *23*, 100194. https://doi.org/10.1016/j.wace.2019.100194

Armitage, S. J., Bristow, C. S., & Drake, N. A. (2015). West African monsoon dynamics inferred from abrupt fluctuations of Lake Mega-Chad. *Proceedings of the National Academy of Sciences*, *112*(28), 8543–8548. https://doi.org/10.1073/pnas.1417655112

Biasutti, M. (2019a). Rainfall trends in the African Sahel: Characteristics, processes, and causes. *WIREs Climate Change*, *10*(4). https://doi.org/10.1002/wcc.591

Biasutti, M. (2019b). Rainfall trends in the African Sahel: Characteristics, processes, and causes. *WIREs Climate Change*, *10*(4). https://doi.org/10.1002/wcc.591

Brandt, M., Mbow, C., Diouf, A. A., Verger, A., Samimi, C., & Fensholt, R. (2015). Ground- and satellite-based evidence of the biophysical mechanisms behind the greening Sahel. *Global Change Biology*, *21*(4), 1610–1620. https://doi.org/10.1111/gcb.12807

Cook, K. H., & Vizy, E. K. (2021). *Hydrodynamics of regional and seasonal variations in Congo Basin precipitation*. Springer Science and Business Media LLC. https://doi.org/10.21203/rs.3.rs-879134/v1

Ehtasham, L., Sherani, S. H., & Nawaz, F. (2024). Acceleration of the hydrological cycle and its impact on water availability over land: An adverse effect of climate change. *Meteorology Hydrology and Water Management*. https://doi.org/10.26491/mhwm/188920

Flamant, C., Knippertz, P., Fink, A. H., Akpo, A., Brooks, B., Chiu, C. J., Coe, H., Danuor, S., Evans, M., Jegede, O., Kalthoff, N., Konaré, A., Liousse, C., Lohou, F., Mari, C., Schlager, H., Schwarzenboeck, A., Adler, B., Amekudzi, L., … Yoboué, V. (2018). The dynamics–aerosol–chemistry–cloud interactions in west africa field campaign: Overview and research highlights. *Bulletin of the American Meteorological Society*, *99*(1), 83–104. https://doi.org/10.1175/bams-d-16-0256.1

Gaetani, M., Janicot, S., Vrac, M., Famien, A. M., & Sultan, B. (2020). Robust assessment of the

https://doi.org/10.5194/egusphere-2026-725
Preprint. Discussion started: 16 February 2026

time of emergence of precipitation change in West Africa. *Scientific Reports*, *10*(1). https://doi.org/10.1038/s41598-020-63782-2

Hersbach, H., Bell, B., Berrisford, P., Hirahara, S., Horányi, A., Muñoz-Sabater, J., Nicolas, J., Peubey, C., Radu, R., Schepers, D., Simmons, A., Soci, C., Abdalla, S., Abellan, X., Balsamo, G., Bechtold, P., Biavati, G., Bidlot, J., Bonavita, M., De Chiara, G., Dahlgren, P., Dee, D., Diamantakis, M., Dragani, R., Flemming, J., Forbes, R., Fuentes, M., Geer, A., Haimberger, L., Healy, S., Hogan, R. J., Hólm, E., Janisková, M., Keeley, S., Laloyaux, P., Lopez, P., Lupu, C., Radnoti, G., de Rosnay, P., Rozum, I., Vamborg, F., Villaume, S., and Thépaut, J.: The ERA5 global reanalysis, Q. J. Roy. Meteor. Soc., 146, 1999–2049, https://doi.org/10.1002/qj.3803 , 2020.

Holloway, C. E., & Neelin, J. D. (2009). Moisture vertical structure, column water vapor, and tropical deep convection. *Journal of the Atmospheric Sciences*, *66*(6), 1665–1683. https://doi.org/10.1175/2008jas2806.1

Janicot, S., Thorncroft, C. D., Ali, A., Asencio, N., Berry, G., Bock, O., Bourles, B., Caniaux, G., Chauvin, F., Deme, A., Kergoat, L., Lafore, J.-P., Lavaysse, C., Lebel, T., Marticorena, B., Mounier, F., Nedelec, P., Redelsperger, J.-L., Ravegnani, F., … Ulanovsky, A. (2008). Large-scale overview of the summer monsoon over West Africa during the AMMA field experiment in 2006. *Annales Geophysicae*, *26*(9), 2569–2595. https://doi.org/10.5194/angeo-26-2569-2008

Johannsen, F., Ermida, S., Martins, J., Trigo, I. F., Nogueira, M., & Dutra, E. (2019). *Cold bias of ERA5 summertime daily maximum land surface temperature over iberian peninsula*. MDPI AG. https://doi.org/10.20944/preprints201909.0268.v1

Kenfack, K., Djiotang Tchotchou, L. A., Marra, F., Bellomo, K., Tamoffo, A. T., Tchana, B. C., Donfack, F. C., Fotso-Nguemo, T. C., Tanessong, R. S., Djomou, Z. Y., & Vondou, D. A. (2025). Radiative anomalies associated with extreme precipitation of November 2023 in equatorial Central Africa. *Atmospheric Research*, *321*, 108090. https://doi.org/10.1016/j.atmosres.2025.108090

Kenfack, K., Marra, F., Yepdo Djomou, Z., Angennes Djiotang Tchotchou, L., Tchio Tamoffo, A., & Appolinaire Vondou, D. (2025). *Dynamic and thermodynamic contribution to the October 2019 exceptional rainfall in West Central Africa*. Copernicus GmbH. https://doi.org/10.5194/egusphere-egu25-347

Lafore, J. P., Biasutti, M., Knippertz, P., & Taylor, C. (2017). The west african monsoon. In *World Scientific Series on Asia-Pacific Weather and Climate* (pp. 35–49). World Scientific. https://doi.org/10.1142/9789813200913_0004

Lavaysse, C., Flamant, C., Janicot, S., Parker, D. J., Lafore, J.-P., Sultan, B., & Pelon, J. (2009). Seasonal evolution of the West African heat low: A climatological perspective. *Climate*

https://doi.org/10.5194/egusphere-2026-725
Preprint. Discussion started: 16 February 2026

Dynamics, *33*(2–3), 313–330. https://doi.org/10.1007/s00382-009-0553-4

Maidment, R. I., Grimes, D., Allan, R. P., Tarnavsky, E., Stringer, M., Hewison, T., Roebeling, R., & Black, E. (2014). The 30 year TAMSAT African Rainfall Climatology And Time series (TARCAT) data set. *Journal of Geophysical Research: Atmospheres*, *119*(18). https://doi.org/10.1002/2014jd021927

Maidment, R. I., Grimes, D., Black, E., Tarnavsky, E., Young, M., Greatrex, H., Allan, R. P., Stein, T., Nkonde, E., Senkunda, S., & Alcántara, E. M. U. (2017). A new, long-term daily satellite-based rainfall dataset for operational monitoring in Africa. *Scientific Data*, *4*(1). https://doi.org/10.1038/sdata.2017.63

Mazhin, S. A., Farrokhi, M., Noroozi, M., Roudini, J., Hosseini, S. A., Motlagh, M. E., Kolivand, P., & Khankeh, H. (2021). Worldwide disaster loss and damage databases: A systematic review. *Journal of education and health promotion*, *10*, 329. https://doi.org/10.4103/jehp.jehp_1525_20

(N.d.). Retrieved January 17, 2026, from https://www.iom.int/sites/g/files/tmzbdl486/files/1028/228493/avis-td-proc-24-02_wash-activities.pdf

Neelin, J. D., & Held, I. M. (1987). Modeling tropical convergence based on the moist static energy budget. *Monthly Weather Review*, *115*(1), 3–12. https://doi.org/10.1175/1520-0493(1987)115<0003:mtcbot>2.0.co;2

Nicholson, S. E. (2013). The west african sahel: A review of recent studies on the rainfall regime and its interannual variability. *ISRN Meteorology*, *2013*, 1–32. https://doi.org/10.1155/2013/453521

Nilsson, E., Becker, P., & Uvo, C. B. (2020). Drivers of abrupt and gradual changes in agricultural systems in Chad. *Regional Environmental Change*, *20*(3). https://doi.org/10.1007/s10113-020-01668-9

OCHA "United Nations Office for the Coordination of Humanitarian Affairs" (2024): TCHAD : Situation des inondations Rapport de situation no03 (01/10/2024).

Parker, D. J., Burton, R. R., Diongue-Niang, A., Ellis, R. J., Felton, M., Taylor, C. M., Thorncroft, C. D., Bessemoulin, P., & Tompkins, A. M. (2005). The diurnal cycle of the West African monsoon circulation. Quarterly Journal of the Royal Meteorological Society, 131(611), 2839–2860. https://doi.org/10.1256/qj.04.52

Pausata, F. S. R., Emanuel, K. A., Chiacchio, M., Diro, G. T., Zhang, Q., Sushama, L., Stager, J. C., & Donnelly, J. P. (2017). Tropical cyclone activity enhanced by Sahara greening and reduced dust emissions during the African Humid Period. *Proceedings of the National Academy of Sciences*, *114*(24), 6221–6226. https://doi.org/10.1073/pnas.1619111114

https://doi.org/10.5194/egusphere-2026-725
Preprint. Discussion started: 16 February 2026

Pausata, F. S. R., Gaetani, M., Messori, G., Berg, A., Maia de Souza, D., Sage, R. F., & deMenocal, P. B. (2020). The greening of the Sahara: Past changes and future implications. *One Earth*, *2*(3), 235–250. https://doi.org/10.1016/j.oneear.2020.03.002

Raymond, D. J., & Jiang, H. (1990). A theory for long-lived mesoscale convective systems. *Journal of the Atmospheric Sciences*, *47*(24), 3067–3077. https://doi.org/10.1175/1520-0469(1990)047<3067:atfllm>2.0.co;2

Romps, D. M. (2015). MSE Minus CAPE is the True Conserved Variable for an Adiabatically Lifted Parcel. *Journal of the Atmospheric Sciences*, *72*(9), 3639–3646. https://doi.org/10.1175/jas-d-15-0054.1

Saha, F., Tchindjang, M., Dzana, J. G., & Nguemadjita, D. (2020). Natural hazards in the Far-North Region of Cameroon and the hydrological extremes dynamics of the Chari-Logone system. Physio-Géo. Physical geography and environment, (Vol. 15), pp69-88. https://doi.org/10.4000/physio-geo.10719

Saha F., Tchio Nkemta D., Tchindjang M., Voundi É. & Mbevo Fendoung P. (2018). Production of so-called “natural” risks in major urban centers of Cameroon, Nat. Sci. Soc., 26 4 (2018) 418-433 DOI: https://doi.org/10.1051/nss/2019003

Selami, N., Sèze, G., Gaetani, M., Grandpeix, J.-Y., Flamant, C., Cuesta, J., & Benabadji, N. (2021). Cloud cover over the Sahara during the summer and associated circulation features. *Atmosphere*, *12*(4), 428. https://doi.org/10.3390/atmos12040428

Seneviratne, S. I., Zhang, X., Adnan, M., Badi, W., Dereczynski, C., Luca, A. D., ... & Allan, R. (2021). Weather and climate extreme events in a changing climate. https://doi.org/10.1017/9781009157896.013

Sindikubwabo, C., Li, R., & Wang, C. (2018). Abrupt change in Sahara precipitation and the associated circulation patterns. *Atmospheric and Climate Sciences*, *08*(02), 262–273. https://doi.org/10.4236/acs.2018.82017

Siwe, A. N., Sandjon, A. T., Tchotchou, L. A. D., Tchinda, C. W., Vondou, D. A., & Nzeukou, A. (2025). Study the impact of intraseasonal oscillations on water vapour transport in central africa: The case of 25–70 day oscillations. *International Journal of Climatology*, *46*(1). https://doi.org/10.1002/joc.70150

Ssenyunzi, R. C., Oruru, B., D’ujanga, F. M., Realini, E., Barindelli, S., Tagliaferro, G., von Engeln, A., & van de Giesen, N. (2020). Performance of ERA5 data in retrieving Precipitable Water Vapour over East African tropical region. *Advances in Space Research*, *65*(8), 1877–1893. https://doi.org/10.1016/j.asr.2020.02.003

Sultan, B., Janicot, S., & Diedhiou, A. (2003). The west african monsoon dynamics. Part I: Documentation of intraseasonal variability. *Journal of Climate*, *16*(21), 3389–3406. https://doi.org/10.1175/1520-0442(2003)016<3389:twamdp>2.0.co;2

https://doi.org/10.5194/egusphere-2026-725
Preprint. Discussion started: 16 February 2026

Tarek, M., Brissette, F. P., & Arsenault, R. (2020). Evaluation of the ERA5 reanalysis as a potential reference dataset for hydrological modelling over North America. *Hydrology and Earth System Sciences*, *24*(5), 2527–2544. https://doi.org/10.5194/hess-24-2527-2020

Tarnavsky, E., Grimes, D., Maidment, R., Black, E., Allan, R. P., Stringer, M., Chadwick, R., & Kayitakire, F. (2014). Extension of the TAMSAT satellite-based rainfall monitoring over Africa and from 1983 to present. *Journal of Applied Meteorology and Climatology*, *53*(12), 2805–2822. https://doi.org/10.1175/jamc-d-14-0016.1

Taylor, C. M., Belušić, D., Guichard, F., Parker, D. J., Vischel, T., Bock, O., Harris, P. P., Janicot, S., Klein, C., & Panthou, G. (2017a). Frequency of extreme Sahelian storms tripled since 1982 in satellite observations. *Nature*, *544*(7651), 475–478. https://doi.org/10.1038/nature22069

Taylor, C. M., Belušić, D., Guichard, F., Parker, D. J., Vischel, T., Bock, O., Harris, P. P., Janicot, S., Klein, C., & Panthou, G. (2017b). Frequency of extreme Sahelian storms tripled since 1982 in satellite observations. *Nature*, *544*(7651), 475–478. https://doi.org/10.1038/nature22069

Tchana, B. C., Djomou, Z. Y., Kenfack, K., Tamoffo, A. T., Mouassom, F. L., Tchotchou, L. A. D., Vondou, D. A., & Mbane, C. B. (2025). Analysis of air temperature anomalies during abnormal rainfall events in Western Central Africa from September to November 2023. *Theoretical and Applied Climatology*, *156*(5). https://doi.org/10.1007/s00704-025-05528-6

Thorncroft, C. D., Bessemoulin, P., & Tompkins, A. M. (2005). The diurnal cycle of the West African monsoon circulation. *Quarterly Journal of the Royal Meteorological Society*, *131*(611), 2839–2860. https://doi.org/10.1256/qj.04.52

Vizy, E. K., & Cook, K. H. (2022). Distribution of extreme rainfall events and their environmental controls in the West African Sahel and Soudan. *Climate Dynamics*, *59*(3–4), 997–1026. https://doi.org/10.1007/s00382-022-06171-x

Vondou, D. A., Maranan, M., Fink, A., & Knippertz, P. (2025). Meteorological conditions leading to a catastrophic, rain-induced landslide in Cameroon in October 2019. Copernicus GmbH. https://doi.org/10.5194/egusphere-egu25-4516

Wainwright, C. M., Finney, D. L., Kilavi, M., Black, E., & Marsham, J. H. (2020). Extreme rainfall in East Africa, October 2019–January 2020 and context under future climate change. *Weather*, *76*(1), 26–31. https://doi.org/10.1002/wea.3824

Wamba Tchinda, C., Tchakoutio Sandjon, A., Djiotang Tchotchou, A. L., Nzeudeu Siwe, A., Vondou, D. A., & Nzeukou, A. (2023). The influence of intraseasonal oscillations on

https://doi.org/10.5194/egusphere-2026-725
Preprint. Discussion started: 16 February 2026

rainfall variability over Central Africa: Case of the 25–70 days variability. *Scientific Reports*, *13*(1). https://doi.org/10.1038/s41598-023-46346-y

Zhang, W., Zhou, T., Ye, W., Zhang, T., Zhang, L., Wolski, P., Risbey, J., Wang, Z., Min, S.-K., Ramsay, H., Brody, M., Grimm, A., Clark, R., Ren, K., Jiang, J., Chen, X., Fu, S., Li, L., Tang, S., & Hu, S. (2025). A year marked by extreme precipitation and floods: Weather and climate extremes in 2024. *Advances in Atmospheric Sciences*, *42*(6), 1045–1063. https://doi.org/10.1007/s00376-025-4540-4